Gross ionization cross sections for rare-gas atoms and simple molecules in 6-MeV/amu fully stripped–ion impact

T. Matsuo,[1] T. Kohno,[2] S. Makino,[2] M. Mizutani,[3] T. Tonuma,[4] A. Kitagawa,[5] T. Murakami,[5] and H. Tawara[6]
[1]*Medical Research Institute, Tokyo Medical and Dental University, 1-5-45 Yushima, Bunkyo-ku, Tokyo 113-8510, Japan*
[2]*Department of Energy Sciences, Tokyo Institute of Technology, 4259 Nagatsuta-cho, Midori-ku, Yokohama 226-8502, Japan*
[3]*Institute for Molecular Sciences, Myodaiji, Okazaki, Aichi 444-8585, Japan*
[4]*RIKEN, 2-1 Hirosawa, Wako-shi, Saitama 351-0198, Japan*
[5]*National Institute of Radiological Sciences, 4-9-1 Anagawa, Inage-ku, Chiba 263-8555, Japan*
[6]*National Institute for Fusion Science, 322-6 Oroshi-cho, Toki, Gifu 509-5292, Japan*
(Received 10 May 1999)

Using the parallel-plate-condenser method, we have measured gross ionization cross sections in fully stripped–ion (charge state $q=2-18$) impact on rare gases and simple molecules (H_2, N_2, O_2, and CO_2) at a fixed collision energy E of 6 MeV/amu. The observed cross sections have been found to depend weakly on the charge state q compared with the q^2 dependence, especially for highly charged projectiles and/or heavy target elements. Therefore, the Bethe-Born calculations tend to overestimate the gross ionization cross sections in multiply charged ion impact at the present collision energy. For a particular target, the gross ionization cross sections have been found to gather on a common curve irrespective of the projectile energy and charge state when the cross section divided by the charge state is plotted against the projectile energy per nucleon divided by the charge state, giving some credence to a scaling law based upon the classical trajectory Monte Carlo (CTMC) method. However, CTMC calculations tend to underestimate the ionization cross sections especially at the high-energy region of $E/q>0.3$ (MeV/amu). A scaling for the gross ionization cross sections of rare gases in fully stripped–ion impact is proposed. [S1050-2947(99)02410-5]

PACS number(s): 34.50.Fa

I. INTRODUCTION

The ionization processes in heavy-ion collisions have been the subject of theoretical and experimental research for a long time. Fast highly charged ion impact is known to be an efficient method to produce cold recoil ions in highly charge states [1]. Besides the interest of multiple ionization as one of the basic collision processes, there are a number of applications for which absolute ionization cross sections of specific targets are necessary. A few such areas are radiation damage in solids, upper atmospheric phenomena, plasma physics, health physics, and particle therapy. Recently have emerged a substantial amount of experimental as well as theoretical studies on absolute values of ionization cross sections in highly charged ion impact. However, there still exist some discrepancies in the dependence of ionization cross sections on the projectile impact energy E or charge state q even in the MeV/amu region.

Olson *et al.* [2] proposed a scaling model for electron-loss processes of hydrogen atoms in highly charged ion impact on the basis of the classical trajectory Monte Carlo (CTMC) method. Similar CTMC calculations coupled with the independent electron approximation were also applied for many electron targets such as rare gases [3]. They were found to be in agreement with most experimental cross-section data for rare-gas targets [4,5], except for those by 4.75 MeV/amu C^{6+} impact reported by Schlachter *et al.* [4], which were consistently larger than other experimental data as well as the calculations by the CTMC model by a factor of 2–4 for all targets studied. These authors also suggested that, in the E/q range from 0.1 to 1.0 MeV/amu, the experimental cross sections change as $q^{3/2}/E^{1/2}$ in contrast to the theoretical prediction of q^2/E [4]. On the other hand, Gillespie [6] calculated the Bethe-Born cross sections for ionization under heavy-ion impact and claimed that the observed cross sections for 4.75 MeV/amu C^{6+} impact [4] are not anomalously too large.

Thus reliable measurements of ionization cross sections in high velocity, highly charged ion impact are still of basic importance, and there is no doubt that additional measurements for absolute cross sections would be necessary in the MeV/amu region. We had previously reported preliminary data for ionization cross sections in collisions of bare projectiles with rare-gas targets measured by a condenser-plate method [7], which provides the so-called gross (or net) ionization cross section σ_g defined as

$$\sigma_g=\Sigma j\sigma_j . \tag{1}$$

Here σ_j is the cross section for producing a recoil (secondary) ion ionized j times. In this study, a set of gross ionization cross sections were measured for He, Ne, Ar, Kr, Xe, H_2, N_2, O_2, and CO_2 targets in collisions of 6 MeV/amu fully stripped ions (He^{2+}, C^{6+}, Ne^{10+}, Si^{14+}, and Ar^{18+}). The results are compared with the data obtained by other experimental groups as well as relevant theoretical calculations.

II. EXPERIMENTAL SETUP AND METHOD

A. Primary beam and target-gas assembly

The present experiment was carried out at the HIMAC (Heavy Ion Medical Accelerator in Chiba) facility of the National Institute of Radiological Sciences (NIRS). Fully stripped projectile ions were accelerated up to 6 MeV/amu

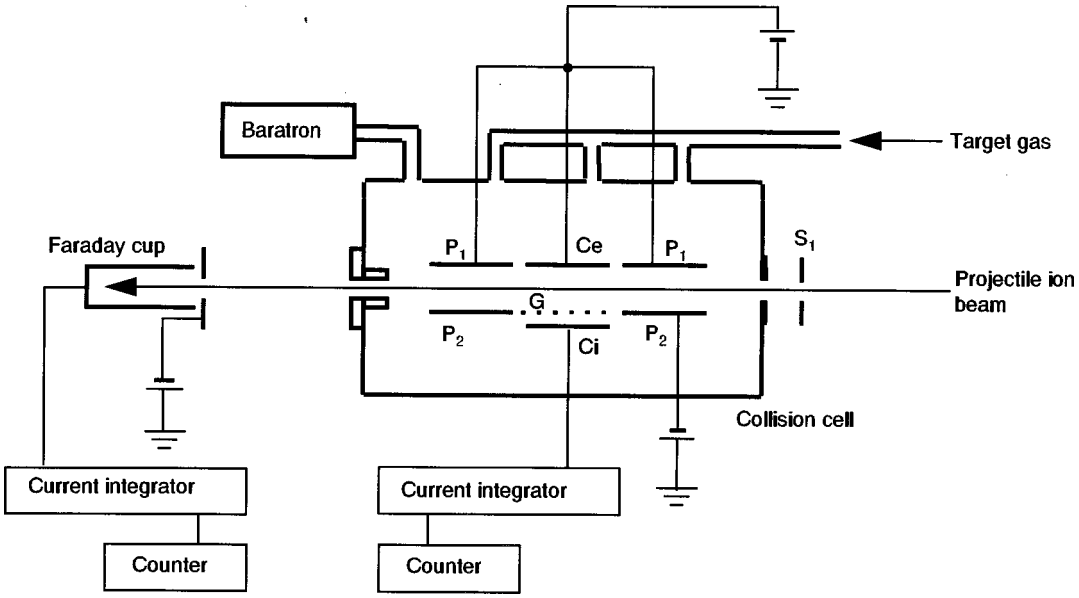

FIG. 1. Schematic diagram of the experimental setup. Ce, electron collection plate; Ci, ion collection plate; G, tungsten wire grid; and S_1, beam defining aperture of 1.5 mm in diameter. A pair of guard plates, P_1 and P_2, are positioned at a distance of 20 mm.

by two (RFQ and Alvarez) linear accelerators. The incident beam was bunched with a width of 700 μs and with a repetition rate of 1–0.5 Hz. The detailed description of the accelerator facility was published elsewhere [8].

Figure 1 shows a schematic diagram of the target gas cell and the condenser-plate assembly used in this experiment, which were modified from those used in a previous experiment by Be *et al.* [9]. The projectile ions entered the target-gas cell through an aperture of 2 mm in diameter after passing a beam-defining aperture of 1.5 mm in diameter. The condenser-plate assembly consists of a pair of parallel plates for collecting ions and a pair of guard plates which provide the uniform electric field for ion collection. After passing through the collision region, the projectile beam was collected in a Faraday cup with a secondary-electron suppresser at -200 V.

The recoil ions produced in collisions arrive at the ion collector plate through a tungsten grid with 92% transmission [9], which prevents the secondary electrons from escaping out of the ion collection plate. In the present measurement, the gross ionization cross sections were deduced from measuring the recoil ion current produced in the collisions. In order to obtain an optimal electric field in the plate assembly, we checked the saturation of the collected recoil ions as a function of the collection field and the electron suppresser potential. The final applied voltage was set to be 0 V (grounded) at the ion collector plate, -20 V at the grid, and $+200$ V at the electron collector plate. The ground potential at the ion collector was chosen so as to directly measure the ion current without an insulation circuit and a current amplifier which may cause additional uncertainty for the cross-section measurement.

The target-gas assembly was installed in a vacuum chamber which was evacuated down to 1×10^{-8} Torr when no target gas was introduced. The target gas was admitted into the collision cell through three pipes at different locations on the upper wall of the cell to provide uniform pressure distributions. The target-gas pressure was kept constant with a pressure control system combined with a capacitance manometer during measurements. The purity of the target gas used in this measurement, as stated by the supplier, was at least 99.99%.

B. Determination of cross sections

The total recoil ion current I_r to the collector plate was measured directly with a digital current integrator. Also the primary beam current I_p was monitored with the Faraday cup using another current integrator. Then current ratios I_r/I_p were determined as a function of the target-gas pressure P whose absolute value was measured with the capacitance manometer (Baratron). The linear relationship between I_r/I_p and P was confirmed over 5×10^{-5} to 1×10^{-3} Torr, indicating that the single collision conditions were satisfied. The gross ionization cross sections were deduced from the slope of the I_r/I_p versus P curve by the least-square fit. We checked that, with the target gas off, the background signals from the ion collection plate were practically zero during typical accumulation periods.

C. Uncertainties

The present gross ionization cross sections might have the following sources of uncertainties: 2% in the effective collision length, 2% in the grid transmission, 5% for the linear least-square fit to the observed data, which includes zero drift and fluctuations in the capacitance manometer and in the current integrator, and 6% in the collection efficiencies of the recoil ions. Combining all of these uncertainties, typical uncertainties in the present gross ionization cross sections are estimated to be within 8.4%. Reproducibility of the measured ionization cross sections was found to be within 2%. It should be noted that, in this study, the gross ionization cross sections were determined by measuring recoil ion currents, a part of which are produced also by electron capture into projectiles, and thus may influence the measured cross sections.

TABLE I. Measured gross ionization cross sections ($\times 10^{-16}$ cm^2).

	He	Ne	Ar	Kr	Xe	H_2	N_2	O_2	CO_2
He^{2+}	0.185	0.524	1.27	1.90	2.98				
C^{6+}	1.58	4.45	10.6	15.9	23.7	2.62	10.2	11.4	15.8
Ne^{10+}	4.11	11.2	26.8	39.3	56.8				36.9
Si^{14+}		19.9	49.0						
Ar^{18+}	11.1	30.7	70.0	98.3	144	19.1	66.4	74.2	99.3

The contribution of such capture processes is, however, estimated to be very small ($< 0.4\%$ to the gross ionization cross section) at the present collision energy.

III. RESULTS AND DISCUSSION

A. Rare-gas targets

1. Dependence of σ_g on q

All of the measured gross ionization cross sections σ_g are summarized in Table I. In Fig. 2, the cross section divided by the square of projectile charge state σ_g/q^2 is plotted as a function of q to illustrate how the cross sections depend on the projectile charge state.

The interaction between a fast ion and a neutral target can be characterized by the Bohr parameter κ, which is defined as follows [10]:

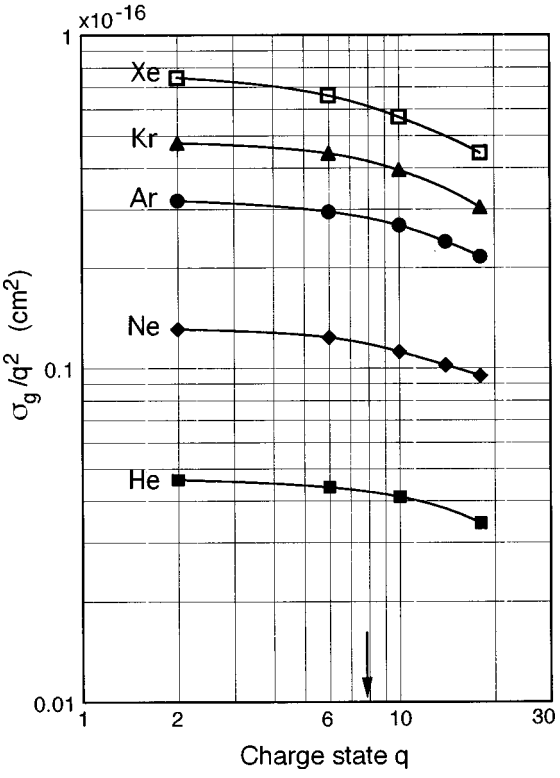

FIG. 2. Gross ionization cross sections divided by the square of projectile charge, σ_g/q^2, as a function of projectile charge q. The arrow indicates the point at which the Bohr parameter becomes unity (see text). Solid curves are drawn for a visual guide.

TABLE II. Calculated values of m assuming a relationship, $\sigma_g \propto q^m$, between gross ionization cross sections σ_g and projectile charge states q. The values of m_1 are obtained from the slope between cross sections for He^{2+} and C^{6+} projectiles and those of m_2 are by the least-squares fitting for the data in C^{6+}-Ar^{18+} projectiles.

	He	Ne	Ar	Kr	Xe
m_1	1.98	1.95	1.93	1.93	1.88
m_2	1.77	1.75	1.72	1.66	1.64

$$\kappa = 2q(v_0/v_p), \tag{2}$$

where v_0 is the Bohr velocity and v_p the projectile velocity. At sufficiently high velocities where $\kappa < 1$, the interaction is brief and weak, and can be described by the perturbation method [10]. The cross section in such approximations is expected to be proportional to q^2 as given by the first Born approximation. On the other hand, if $\kappa > 1$, the perturbation treatment is not valid any more. In the present collision energy, values of κ range from 0.26 to 2.33 for He^{2+}-Ar^{18+} projectiles. In He target, the cross sections for He^{2+} and C^{6+} projectiles seem to follow closely the q^2 dependence. On the other hand, in heavier projectiles such as Ne^{10+}, Sl^{14+}, and Ar^{18+}, where κ is larger than unity, the reduced cross section σ_g/q^2 markedly decreases as the projectile charge increases.

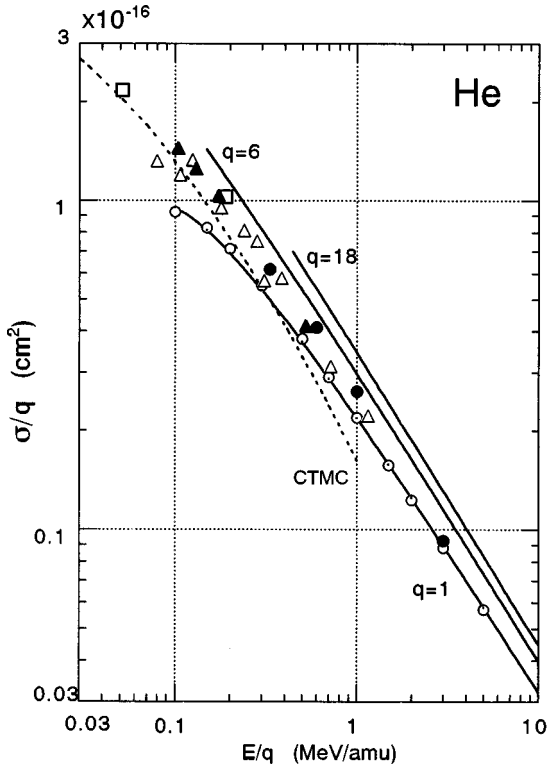

FIG. 3. Reduced plot of He ionization cross sections for a bare projectile ion with charge state q. ●, present results; ▲, He^{2+}, C^{6+}, O^{8+}, and Ne^{10+} impact by Be *et al.* [9]; □, C^{6+} by Schlachter *et al.* [4]; △, He^{2+}, O^{6+}, and O^{8+} by Knudsen *et al.* [10]; and ○, H^+ by Rudd *et al.* [12]. The dotted curve shows CTMC cross sections for the gross ionization reported by Schlachter *et al.* [4]. Solid curves show Bethe-Born cross sections for projectile charges $q = 1$, 6, and 18 as indicated (see text).

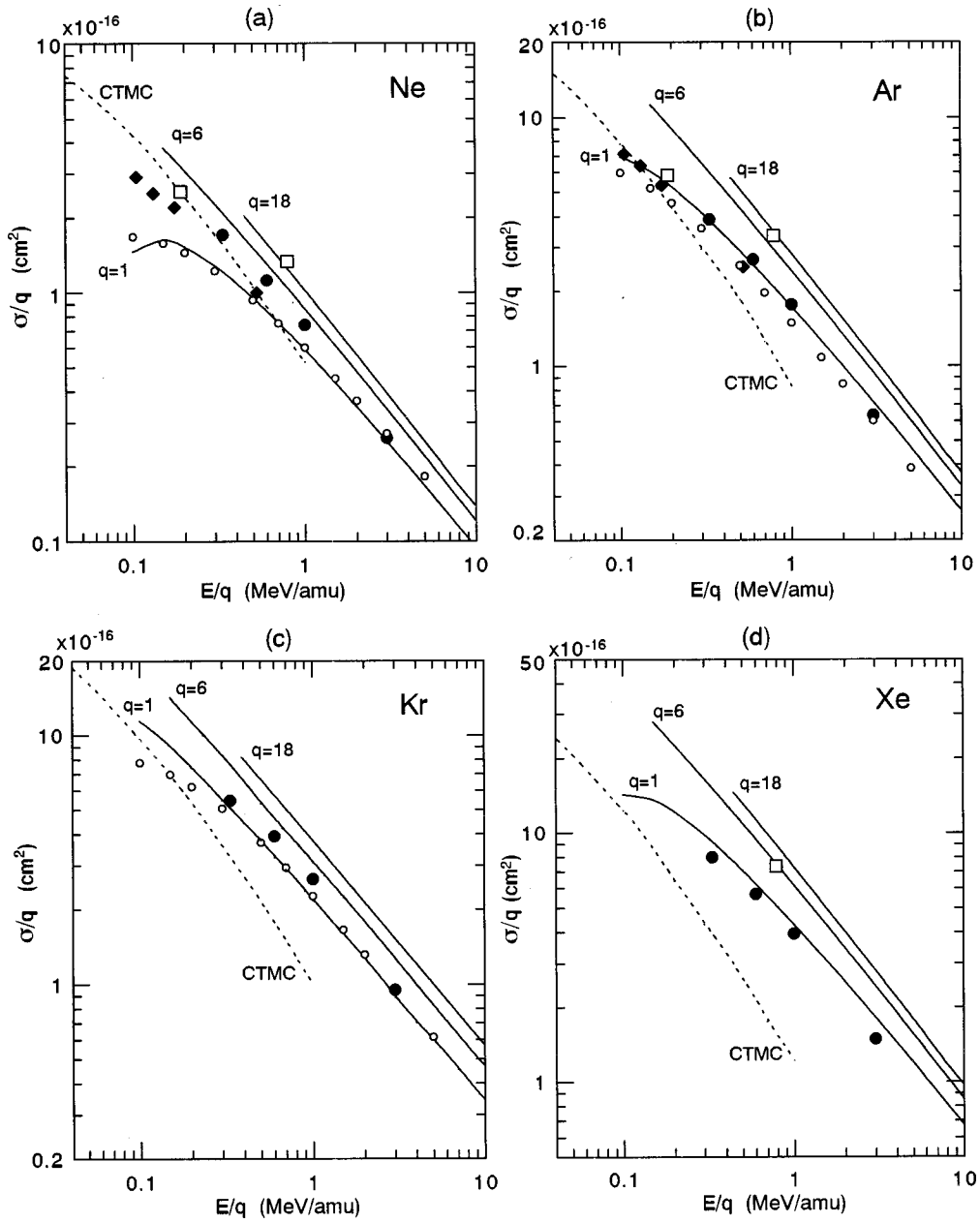

FIG. 4. Reduced plot of ionization cross sections for a bare projectile ion with charge state q in rare-gas targets: (a) Ne, (b) Ar, (c) Kr, and (d) Xe. ●, present results; ◆, He^{2+}, C^{6+}, O^{8+}, and Ne^{10+} impact by Be *et al.* [9]; □, C^{6+} by Schlachter *et al.* [4]; and ○, H^{+} by Rudd *et al.* [12]. The dotted curve shows CTMC cross sections for the gross ionization reported by Schlachter *et al.* [4] and the solid curves show the Bethe-Born cross sections for projectile charges $q=1$, 6, and 18 as indicated (see text).

To illustrate this problem quantitatively, the observed cross sections were fitted to a power-law dependence on the projectile charge state, namely $\sigma_g \propto q^m$ [9]. Then m values for C^{6+}-Ar^{18+} projectiles were determined by the least-square fit. Also the m values were calculated from the slope between He^{2+} and O^{6+} projectiles. The results are given in Table II. As expected, the m value for the He target in light ion impact is close to 2. On the other hand, in heavy projectile ions, the deviation from the q^2 dependence is significant. It is also noted that, as the target becomes heavier, the cross sections deviate from the q^2 dependence even in light ion impact. This is due to the fact that multiple ionization becomes important for heavier target atoms.

2. Comparison to other experimental cross sections and the CTMC scaling

Schlachter *et al.* [4] used the CTMC method coupled with the independent-electron approximation to calculate gross ionization cross sections in rare gases for projectiles with charge states from +5 to +80 in the energy range of 1–5 MeV/amu and showed that, for a given rare-gas target, gross ionization cross sections can be reduced to a common curve in the scaled coordinates, namely $\log_{10}(\sigma_g/q)$ versus $\log_{10}(E/q)$. In Fig. 3, we plot the present results for the He target, and those for other rare gases in Figs. 4(a)–4(d). In these figures, gross ionization cross sections for fully stripped projectile ions reported by other investigators

[4,5,9–11] as well as those in proton impact by Rudd *et al.* [12] are also plotted for comparison. It can be seen that the experimental cross sections show reasonable agreement with each other, except the data at 4.75 MeV/amu C^{6+} impact ($E/q=0.79$) by Schlachter *et al.* [4], which are too large compared with other experimental data, as mentioned already.

The CTMC results for gross ionization cross sections are also reproduced with the broken curves in Figs. 3 and 4. For a given target species, all the measured cross sections, except for the data at 4.75 MeV/amu C^{6+} impact, seem to lie around a single curve irrespective of the projectile energy and charge state, supporting the scaling predicted by the CTMC calculations. However, one can also note that the CTMC calculations become smaller than the experimental values at high E/q. The heavier the target, the larger the difference between experimental and the CTMC results becomes. For example, in the Xe target, the present cross sections are 2.4–3.8 times larger than those calculated by the CTMC method.

3. Comparison with the Born calculation

The theoretical treatment of inelastic collisions between fast charged particles with atoms and molecules has been described in detail by Inokuti [13]. Gillespie [6] has pointed out that, at sufficiently high projectile velocities v, the inelastic cross sections σ under structureless ion impact can be calculated based on the Bethe-Born approximation in the form

$$\sigma=4\pi a_0^2\frac{\alpha^2}{\beta^2}q^2\left[M^2\left(\ln\frac{\beta^2}{1-\beta^2}-\beta^2\right)+C+\gamma\frac{\alpha^2}{\beta^2}\right], \quad (3)$$

where a_0 is the Bohr radius, α the fine-structure constant, c the velocity of light, and $\beta=v/c$. The other parameters M^2, C, and γ are constants depending on the atomic properties of the target under consideration.

It should be mentioned here that the experimental measurements and theoretical calculations do not always address the same quantity. In theory, it is common to calculate either the partial ionization cross section for a particular state σ_j or the total (or counting) ionization cross section σ_t, which is given by

$$\sigma_t=\Sigma\sigma_j\,. \quad (4)$$

Clearly, the gross ionization cross section σ_g given by Eq. (1) should be larger than the total ionization cross section σ_t. Also, the total inelastic cross section σ_j (total ionization plus all discrete excitation) can be calculated using Eq. (3). For rare gases, σ_g is expected to be close to $\sigma_{\rm in}$ because the discrete excitation probabilities are expected to be very small, compared with those of ionization, in high-energy collisions [6].

Using the parameters (M^2, C, and γ) given in the paper of Gillespie [6], we calculated the total ionization cross sections σ_t for He and Ne, and $\sigma_{\rm in}$ for Ar and Xe using Eq. (3) for projectile charges $q=1$, 6, and 18. Total ionization cross sections σ_t in the Kr target were scaled from the Born cross sections in proton impact calculated by McGuire [14]. In Figs. 3 and 4, the solid curves representing the Born calculations are drawn in the energy range $(q\alpha/\beta)^2\leqslant 1$, where the Born approximation is thought to be valid [6].

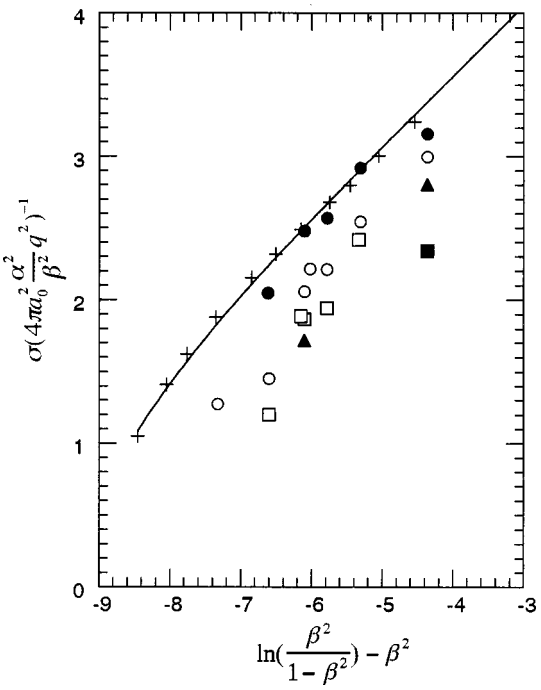

FIG. 5. Fano plots for ionization of He. The solid curve is the Bethe-Born results calculated using parameters given by Gillespie [6]. Symbols are gross ionization cross sections for the impact of fully stripped ions reported by different experimental groups [4,9,10,12]. Experimental data are grouped according to the projectile species as denoted by symbols: +, H^+; ●, He^{2+}; ○, C^{6+}; □, O^{8+}; ▲, Ne^{10+}; and ■, Ar^{18+} impact.

As can be noted in Figs. 3 and 4, we obtain a family of curves of the Born calculations for projectile charges $q=1-18$ rather than a single curve suggested by the CTMC results. It is also noted that the Born cross sections for highly charge projectiles (6+ and 18+) are significantly large compared with the experimental results, although those for proton impact show an excellent agreement with experiments. This is understood from the fact that the observed gross ionization cross sections scale weaker than q^2 in heavy projectile impact as discussed in Sec. III A 1.

4. Fano plot for He

In the MeV/amu energy region, there are copious measured cross-section data for the He target compared with those for heavier rare gases. Recently, Berg *et al.* [15] have reported that the He single ionization cross sections σ_+ in highly charged ($q=24-92$) ion impact fall reasonably close to a universal curve over a wide range of collision energy ($E=3.6$ MeV/amu–1 GeV/amu) when σ_+/q is plotted against E/q, similar to Fig. 3. However, the scaling rule might be subtle for lower projectile charges as in the present measurement.

To illustrate the situation clearly, a Fano plot for gross ionization cross sections of He is shown in Fig. 5, in which experimental data cited in Fig. 3 are replotted. The cross sections are marked according to the projectile charge state. Although the data points are considerably scattered, those for different projectile charge groups are distinguishable from

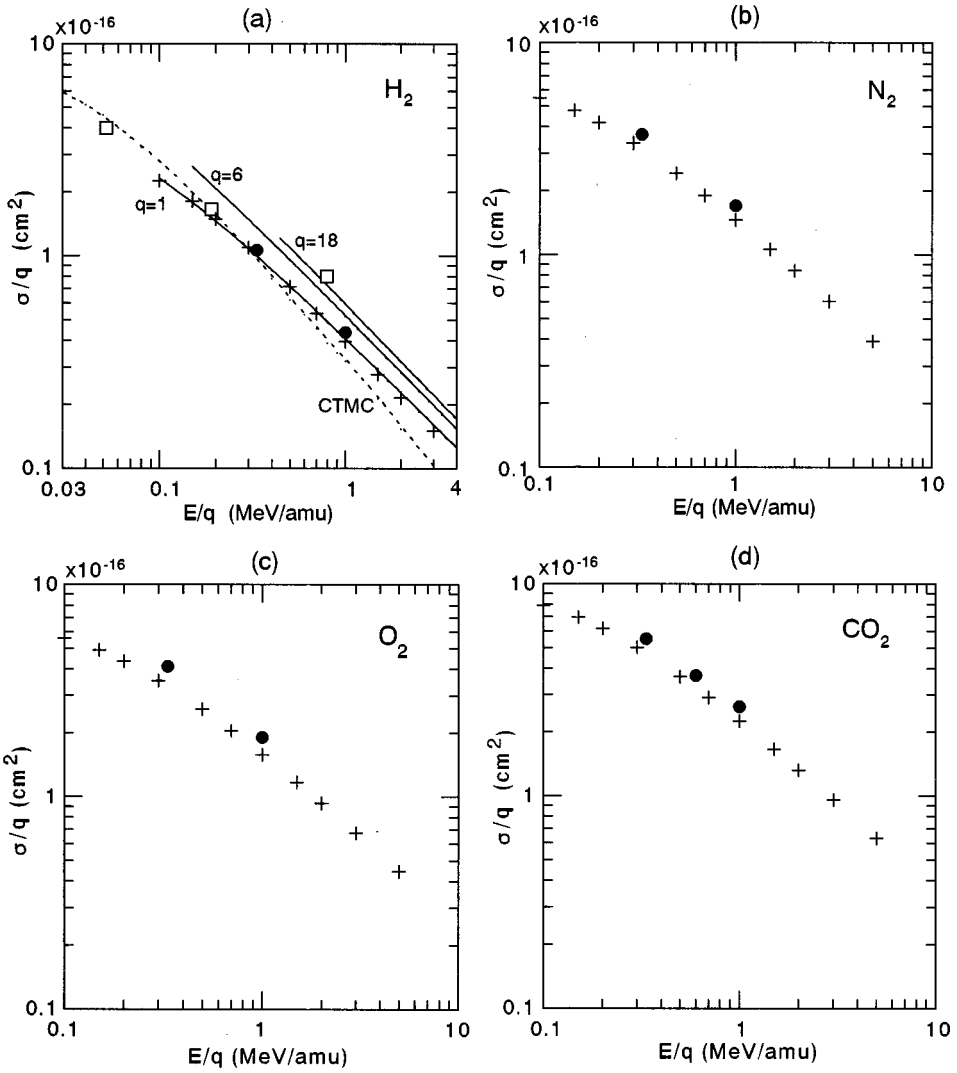

FIG. 6. Reduced plot of the ionization cross sections vs collision energy for molecules. ●, present results; +, H^+ impact by Rudd *et al.* [12]; and □, C^{6+} by Schlachter *et al.* [4]. The dotted curve shows CTMC results by Olson *et al.* [2] and the solid curves show Bethe-Born cross sections for projectile charge $q=1$, 6, and 18 as indicated.

each other. As the projectile charge increases from 2+ to 18+, the data points systematically deviate from the theoretical curve of the Bethe-Born approximation. This shows that, apart from the simple scaling, further systematic cross-section measurements and refined theoretical studies are required in order to gain detailed understanding of He ionization in relatively low $q(\leqslant 18)$ bare-ion collisions.

B. Molecular targets

The measured gross ionization cross sections for H_2, N_2, O_2, and CO_2 are also summarized in Table I. The relationships between σ_g/q and E/q for molecular targets are represented in Figs. 6(a)–6(d). Unfortunately, theoretical calculations as well as experimental data for molecular targets are still scarce in high-energy heavy-ion impact except for the H_2 target.

Figure 6(a) shows the present results for H_2 molecules in comparison to other experimental data by bare heavy-ion impact as well as by proton impact. The broken curve shows twice the gross ionization cross sections for a hydrogen atom calculated by the CTMC method [2]. Total ionization cross sections of H_2 for projectiles with charge states $q=1$, 6, and 18 were also calculated with Eq. (3) using the parameters given in the paper of Gillespie [6]. As can be noted, the experimental data from fully stripped-ion impact lie slightly above those by proton impact. Except for the cross section at 4.75 MeV/amu C^{6+} impact ($E/q=0.79$) [4], which is again anomalously large, the experimental data seem to lie around a single curve with only slight scattering and thereby show agreement with the CTMC calculations below E/q <0.5 MeV/amu. At the higher E/q region, CTMC cross sections tend to decrease more rapidly than the experimental results, as observed in rare gases. Again, the Bethe-Born theory overestimates cross sections for highly charged projectiles.

As shown in Figs. 6(b)–6(d), the present scaled cross sections for N_2, O_2, and CO_2 molecules under heavy projectile impact seem to follow nicely those in proton impact reported by Rudd *et al.* [12].

C. A scaling for rare-gas targets

It might be useful to have scaling laws which provide simple and accurate estimate for ionization cross sections for

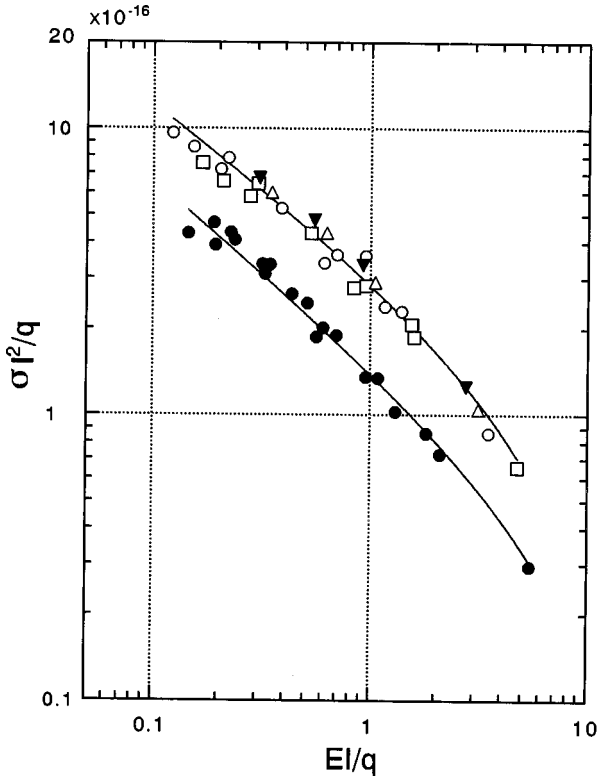

FIG. 7. Gross ionization cross sections for rare gases from different experiments [4,7,9,10,11] are plotted in the reduced coordinates ($\sigma_g I^2/q$ vs EI/q). Here the mean ionization potential I is taken to be the weighted mean value of the first two ionization energies corresponding to the $^2P_{3/2}$ and $^2P_{1/2}$ states of a singly charged ion. E is in MeV/amu, I in Rydberg units, and σ_g in $10^{-16}\,\mathrm{cm}^2$. Experimental cross sections are grouped according to target species: ●, He; □, Ne; ○, Ar; △, Kr; and ▼, Xe. The solid curves are drawn for a visual guide.

various combinations of collision partners over a wide range of the projectile ion energy and charge state. We propose here a scaling for ionization of rare gases in fully stripped-ion impact. In Fig. 7, the present gross ionization cross sections and those from other experiments are plotted in the reduced coordinates ($\log_{10}(\sigma_g I^2/q)$ versus EI/q). Here, please refer to I is the mean ionization potential of the target in Rydberg units, which is taken to be the weighted mean value of the first two ionization energies corresponding to the $^2P_{1/2}$ and $^2P_{3/2}$ states of a singly charged ion.

It should be noted that the reduced cross sections for Ne, Ar, Kr, and Xe are distributed around a common curve and those for He fall well on another curve. The difference between He and other rare gases can be ascribed to the number and properties of the outermost electron shell; i.e., two $1s$ electrons in He and six np electrons in other rare gases. When the cross sections for Ne, Ar, Kr, and Xe were divided by 2, they were found to be reduced on the curve of He. This suggests the following scaling:

$$\sigma_g I^2/q = n f(EI/q). \tag{5}$$

Here n is the effective number of electrons in the outermost shell under consideration. Although the theoretical background or the physical meaning of this scaling law is not clear at present, we have confirmed that a quite similar situation holds true in the Born ionization cross sections for proton–rare-gas collisions (to appear in a subsequent paper).

IV. CONCLUDING REMARKS

We have determined the absolute values of gross ionization cross sections for rare gases and simple molecules in collisions of 6 MeV/amu fully stripped ions with charge states $q=2-18$. By comparing the obtained results with relevant theories and other experiments, the anomaly in the energy/charge dependence of ionization cross sections reported previously has been corrected. The present E/q values seem to be in marginal regions for available theoretical treatments; i.e., the upper limit of the CTMC method and the lower limit for the Born approximation. The measured cross sections are found to be varied more weakly than the q^2 dependence, indicating the failure of the first Born approximation even at the present collision energy (6 MeV/amu). The CTMC results tend to underestimate the cross sections, although the scaling law predicted by this method seems to be roughly consistent with the experiments. A scaling law for ionization cross sections of rare gases is proposed, in which the ionization potential of the target and the effective number of electrons involved in the ionization are included as parameters in addition to the projectile energy E and the charge state q. Further sophisticated measurements and theoretical studies for various combinations of collision partners would be highly desirable in order to understand the detailed ionization mechanisms in energetic multiply charged ion collisions.

ACKNOWLEDGMENTS

This work was performed as part of the Research Project with Heavy Ions at NIRS-HIMAC. We would like to thank the HIMAC crew for providing excellent beams, and Tsuyoshi Kato and Takashi Kamiya for their technical support.

[1] C. L. Cocke and R. E. Olson, Phys. Rep. **205**, 153 (1991).
[2] R. E. Olson, K. H. Berkner, W. G. Graham, R. V. Pyle, A. S. Schlachter, and J. W. Stearns, Phys. Rev. Lett. **41**, 163 (1978).
[3] R. E. Olson, J. Phys. B **12**, 1843 (1979).
[4] A. S. Schlachter, K. H. Berkner, W. G. Graham, R. V. Pyle, P. J. Schneider, K. R. Stalder, J. W. Stearns, J. A. Tanis, and R. E. Olson, Phys. Rev. A **23**, 2331 (1981).
[5] A. S. Schlachter, K. H. Berkner, H. F. Beyer, W. G. Graham, W. Groh, R. Mann, A. Müller, R. E. Olson, R. V. Pyle, J. W. Stearns, and J. A. Tanis, Phys. Scr. **T3**, 153 (1983).
[6] G. H. Gillespie, Phys. Rev. A **24**, 608 (1981).
[7] S. Makino, T. Matsuo, M. Mizutani, M. Sano, T. Kohno, T. Tonuma, H. Tawara, A. Kitagawa, and T. Murakami, Phys. Scr. **T73**, 238 (1997).
[8] Y. Hirao *et al.*, NIRS Report No. NIRS-M-89/HIMAC-001 (1992).

[9] S. H. Be, T. Tonuma, H. Kumagai, H. Shibata, M. Kase, T. Kambara, I. Kohno, and H. Tawara, J. Phys. B **19**, 1771 (1986).
[10] H. Knudsen, L. H. Andersen, P. Hvelplund, G. Astner, H. Cederquist, H. Danared, L. Liljeby, and K-G. Rensfelt, J. Phys. B **17**, 3545 (1984).
[11] A. Cassimi, J. P. Grandin, and L. H. Zhang, Radiat. Eff. Defects Solids **126**, 21 (1993).
[12] M. E. Rudd, R. D. Dubois, L. H. Toburen, C. A. Ratcliffe, and T. V. Goffe, Phys. Rev. A **28**, 3244 (1983).
[13] M. Inokuti, Rev. Mod. Phys. **43**, 279 (1971).
[14] E. J. McGuire, Phys. Rev. A **22**, 868 (1980).
[15] H. Berg, J. Ullrich, E. Bernstein, M. Unverzagt, L. Spielberger, J. Euler, D. Schardt, O. Jagutzki, H. Schmidt-Böcking, R. Mann, P. H. Mokler, S. Hagmann, and P. D. Fainstein, J. Phys. B **25**, 3655 (1992).